Effects of geological characteristics on the kinematics of historical Hungtsaiping landslide

Wei-Kai Huang [1] Chia-Ming Lo [2] Ming-Lang Lin [3] Jia-Jyun Dong[4] Kuang-Tsung Chang [5] Yu- Lin Chang [6]

[1] Geotechnical Engineering Research Center Research Assistant

[2] Department of Civil Engineering, Graduate Institute of Civil and Disaster Reduction Engineering, Chienkuo Technology University Assistance Professor

[3] Department of Civil Engineering, National Taiwan University Professor

[4]Graduate Institute of Applied Geology, National Central University Professor

[5]Department of Soil And Water Conservation, National Chung Hsing University Associate Professor

[6] Geotechnical Engineering Research Center Deputy Manager

Abstract

The Chi-Chi earthquake triggered a large, 100 hectare, deep-seated landslide in the Huangtsaiping area of Nantou county in 1999. Through field investigations, an irregular pattern of displacement vectors was identified, making this failure very complex. Landslide site investigations included field reconnaissance, geomorphologic analysis, geophysical exploration, borehole logs, and laboratory experiments. The Hungtsaiping area exhibited at least three large landslide events, two ancient rockslides (the first triggered during the 1916 Nantou earthquake and other event occurring after 1934) and the 1999 colluvium slide (triggered during the 1999 Chi-chi earthquake). With the consideration of a source collapse mass, three landslide events were reasonably reproduced using a 3D discrete element model. The numerical model parameters were calibrated using rock mass strength behavior and the morphology of the landslide deposits.

Keywords: Geological characteristics, Landslide, 3D discrete element modeling.

1. Introduction

The Chi-Chi earthquake, which occurred on September 21, 1999 with the Richter magnitude of 7.3 and its epicenter at Chi-Chi city, triggered more than 9000 landslides over 128 km2 in the central mountain area of the island (Liao, 2000). Nantou county was the most seriously affected, where several fast and catastrophic landslides occurred, such as the Jiufengershan and Tsaoling landslide. On the other hand, a slow deep-seated landslide induced by the earthquake was noticed at Hungtsaiping in Nantou county (Lee et al., 2004; Wei and Lee, 2006). Deep-seated mass movements are not well understood due to their large scale of deformation, limited applicability and the cost of ground surveys. However, several large gravitational failure cases have been described that highlight the importance of landslide kinematics (e.g. Chang et al., 2005; Dong et al., 2009; Lo et al., 2011). Moreover, large, high velocity landslides, especially the disintegrative rockslides that develop into debris avalanches (sturzstroms) are remarkable geological phenomena (Steven and

Simon, 2006). Deep-seated landslides in Huntsaiping are commonly covered by colluvium that was caused by ancient landslides (Chang et al., 2008; Lo et al.,2008). The mechanism of the Huntsaiping landslide was complex. That caused the kinematics and geomorphology development to be very difficult to interpret for each event.

Dong (2009) concluded that the seismic anisotropy, sliding direction, and mechanical properties of the sliding surfaces are important contributing factors to the kinematics of a landslide. However, the complex kinematics of Hungtsaiping landslide need appropriate numerical analysis to simulate the movement process for each event. This understanding of the landslide mechanism and kinematics will be helpful for mitigation strategies, or for prediction of possible future landform processes.

In view of this, in order to simulate the sliding material, because field investigation noticed the landslides often involve heterogeneous granular materials such as rocks and debris, the discrete element method is appropriate for the analysis of the sliding process, and also the authoritative tool to simulate the kinematics of landslide movement (e.g. Chang et al., 2005; Tang et al., 2009; Lo et al.,2011). Chang (2011) used 2D discrete element model and concluded the model can reasonably reproduce the ancient rock slide and the 1999 colluvium slide at Hungtsaiping, but the runout of the ancient rockslide was only considered in a straight path due to the 2D topographic effects, which neglected the diffusion characteristic for the 3D complexity of the terrain in Hungtsaiping.

To summarize the above conclusions, the complex slope collapse mechanism of the sliding mass depends on the morphological and geological characteristics, the rheology of sliding materials, and the triggering condition. Thus, the study described the geological characteristics in the Hungtsaiping during the Nantou earthquake (1916) and Chi-chi earthquake (1999) events using a 3D discrete element model based on the theory of granular mechanics with the aim of:

(a) simulating the movement process of the Hungtsaiping landslide for each event during earthquake events.
(b) establishing the relationship between the geological characteristics and the landslide kinematics.

2. TERRAIN OF THE HUNGTSAIPING LANDSLIDE

The evidence from the geomorphic features provided the activity of past landslides and potential unstable zones. Furthermore, topographic maps show the size, shape, and depiction of the landslide area. The orthographic topographic maps, at scales of 1:20000, 1:25000 and 1:50000 released in 1904, 1934, 1998, 2003 respectively, were used to interpret the geomorphic features of the landslides (Fig.1). The Yonglu stream played a crucial role in the study area. The Nantou series of earthquake events (1916-1917) caused the first landslide between 1904 and 1934. The sliding mass deflected the Yonglu stream toward northwest. This event caused the toe of sliding mass III to daylight and the instability that provided conditions for the dip slope failure after 1934. Chi-chi earthquake caused sliding mass I and III slip displacements of about 28 meters in 1999 (Lee et al., 2004).

3.GEOLOGY INVESTIGATION AND BOREHOLE LOGS OF THE HUNGTSAIPING

The geological map of Hungtsaiping area is the main reference for the simulation model based on geology investigation shown in Fig. 2. The axis of the syncline was constrained by the measured orientation of the bedding planes. M-symmetry minor folds of thin-bedded siltstone and sandstone layers within a massive shale (Tanliaoti Shale) crop out on the river bank of Yonglu stream (Fig.2 a), and these M folds should coincide with the hinge of a large fold structure (Dong et al., 2009).

According to results of borehole logs and RIP (resistivity image profiling) (Fig.2b), the interface between the shale and the colluvium was mainly a bedding plane. Before the 1999 colluvium slide, an ancient rockslide was speculated to be the cause the thick colluvium. The possible source is the massive sandstone exposed at the southeast of the slide area, where the current sandstone appears as scarps and steep slopes. The ancient rock mass, composed mainly of sandstone might have slid along a surface that was in the underlying shale under certain unstable conditions, such as those caused by rain or an earthquake (Chang et al., 2011).

Comprehensive results of the geology investigation and borehole logs survey and mapping of the underlain strata of Hungtsaiping landslide are shown in Fig.2c. The numerical modeling reconstructed the past landslide process during earthquake events based on the geological map, which is helpful for explaining the effect of geological characteristics on the kinematics of Hungtsaiping landslides.

4.3D NUMERICAL MODEL OF THE HUNGTSAIPING LANDSLIDE

PFC (Particle Flow Code) was implemented using the Discrete Element Method proposed by Cundall and Strack (1979). This technique is commonly used for the modeling of granular assemblages with purely frictional or bonded circular particles represented by discs in two dimensions. The original version of the Discrete Element Method was devoted to the modeling of rock-block systems (Cundall, 1971). It was later applied to the modeling of granular material (Cundall and Strack, 1979). The Discrete Element Method does not limit the scale of separation and displacement behaviors of elements, and the movement process of the mass from fracture to separation can be fully simulated, so it is very applicable to the simulation of landslides (Poisel and Roth, 2004; Poisel et al., 2005). Hence this paper used PFC 3D to simulate and interpret the kinematic process of Hungtsaiping landslides for three events. The elements of the PFC model mainly include particles and walls. The sliding surface of the collapse area in the Hungtsaiping landslide model was constructed by 87,000 wall elements based on a 15×15m DEM from the mapping of underlain strata and geologic structure. An attempt to reconstruct the geological structure sliding surface before the 1904 Nantou series earthquake events is shown in (Fig.3a). The total length from east to west was 3,765m, and the total width from south to north was 2,625m. The sliding mass of the Hungtsaiping landslide was constructed using 20,158 spherical elements with a radius of 7.5 meters and the 18,379 spherical elements were divided into three blocks (Fig.3b, 4a); the total volume was about 33 million cubic meters.

The macroscopic behavior of the granular media depends on the contact mechanical properties, but there is no straightforward solution relating these parameters. To use PFC models as reliable simulation tools, it is necessary to establish reasonable relations between the numerical parameters and the mechanical characteristics of real problems (Potyondy and Cundall, 2004). Recently, application of experimental design and optimization to PFC model calibration in uniaxial compression test was proposed to calculate proper macro-parameters for model generation in order to closely reproduce macro-parameters of the rock material such as uniaxial compression strength (UCS), Young's modulus and Poisson's ratio (Yoon, 2007). For the bond model, the macro-parameters for interaction of two circular particles are normal and shear stiffness. Normal and shear bonds, and the Coulomb friction coefficient must be obtained during the calibration step. Fakhimi (2004) proposed a slightly overlapped circular particle interaction to resolve the failure envelope and the ratio of unconfined compressive strength to tensile strength which is usually lower than that of a rock. An application of dimensional analysis in the calibration of a discrete element method for sandstone was carried out to mimic the deformational and failure characteristics in stress paths (Fakhimi and Villegas, 2007). Although there is no straightforward solution from

micro-properties to macro-parameters, some relations exist between the two properties for initial calibration as follows. The Young's modules of the grains and cement are expressed by:

$$E_c = \frac{k_n}{4R} \qquad [1]$$

Where kn and R are particle normal stiffness and particle radius (Potyondy and Cundall, 2004). Thus, Poisson's ratio depends both on the ratio of shear contact stiffness to normal contact stiffness and packing geometry. The peak strength of the material depends both on the friction coefficient and the bond strength (Itasca, 2002).

Thus we performed a series of compression numerical tests on granular samples to derive the rock mechanical macro-properties, and took a field investigation sample (Fig.5a., b.) to modify strength properties of Hungtsaiping sandstone borehole logs result (Chang et al., 2011) by the Hoek–Brown failure criterion (Fig.5 c., d.). The 3D granular sample consists of 8574 spherical elements. The numerical parameters obtained for a compression test are the Young's modulus E=407.21MPa, and the compression strength UCS=5.249MPa. The internal friction angle is 17.63° (Fig.5e). The macroscopic properties of the numerical sample are similar to the properties of the rock samples from the sandstone, as determined from laboratory tests (Tab.1). Tab.2 is the numerical parameters used for PFC modelling.

The numerical model of the Hungtsaiping landslide was reconstructed into three landslide events that are explained as follow:

1. First landslide event: The Nantou series of earthquake events caused the first landslide between 1904 and 1934, which possibly caused the massive sandstone exposure at the southeast of the slide area, where the current sandstone appears as scarps and steep slopes (mass A, mass B, and mass C). According to the simulation result, this was triggered during the 1904 to 1934 Nantou series of earthquakes. In this case, that gave the gravitational impetus to the simulated landslide after the earthquake events while the rock mass C was in movement, the mass B slide almost entirely collapsed, causing the thick colluviums that deflected the Yonglu stream toward northwest (Fig.4b).
2. Second landslide event: After the Nantou series of earthquake events caused the first landslide, mass B and mass C, triggered by ground motion, caused mass A to loose support, and collapse under the influence of gravity (Fig.4c, d).
3. Chi-chi earthquake event: The ancient landslide model which results in deposition at the down slope, continues for the simulation of the 1999 landslide. The deposit in the creek valley is eliminated as the result of the geological process of erosion before the earthquake. The strong motion records collected at the station TCU072 (Fig.6), which is 10 km away, are used for earthquake loading (Fig.4e). Using the ball elements of sliding mass to record sliding displacement, the maximum displacement is 25.6 m, and the displacement of elements is shown in Fig.7.

5. DISCUSSION AND CONCLUSIONS

The Discrete Element numerical modeling of the three event-caused landslides brings important physical constraints that can be compared with, and controlled by, field observations and reported disaster characteristics of those events. The research on the Nantou series of earthquakes, the Chi-Chi earthquake (Lo et al.,2008; Chang et al.,2011; Lee et al., 1999) and earlier studies associated with those earthquakes provided abundant background information to explore the possible factors that govern the kinematics of the large earthquake-induced landslides. Based on previous studies to build numerical simulation, we can discuss in more detail the possible reasons for slide mass movement after the events. When the simulation results from PFC3D were compared with the particle image velocimetry technology (PIV) (Lo et al.,2008) in Chi-Chi earthquake event,

the boundary and movement direction of colluvium almost matched (Fig.8), and therefore had same conditions worth exploring. In the field, we found evidence of a Syncline, that is M-symmetry minor folds of thin-bedded siltstone and sandstone layers within a massive shale (Tanliaoti Shale) crop out on the river bank of Yonglu stream, which played a crucial role for this study area. It controlled sliding direction and, after the Nantou series of earthquakes, let the sliding mass (Fig.4b mass B, mass C) turn northwest to north and deflected the Yonglu stream toward northwest between 1904 to 1934. This event caused the toe of sliding mass A to daylight and destabilize, which provided conditions for the dip slope failure after 1934. Chi-chi earthquake caused sliding mass A, B, and C slip displacement of about 25.61 meters between 1998 to 2003. The conditions of this case are worth discussing.

In the simulation, the area of ball ID 2020 and 2037 around had a large displacement of about 19.1 m. On the other hand, the area of ball ID 7289 and 7756 around at the lower slope that only had a displacement of about 1.48 m. The existence of such large differences in displacement may have caused deformation of the mass of colluvium and resulted in tension cracks developing on the sliding surface.

The discrete element method is suitable for the modeling of landslides with long runout provided that the determination of the micro-parameters can be reasonably solved for the mechanical behavior of the geomaterials on slopes.

REFERENCES

1. Chang KJ, Taboada A, Chan YC (2005) Geological and morphological study of the Jiufengershan landslide triggered by the Chi-Chi Taiwan earthquake. Geomorphology 71(3-4):293-309.
2. Chang KT, Lai CC, Lin DG (2008) Analyses of the Huntsaiping Landslide Induced by the Chichi Earthquake, Journal of Chinese Soil and Water Conservation, 39(3): 329-344 (in Chinese).
3. Chang KT, Lin ML, Dong JJ, Chien CH (2011) The Hungtsaiping landslides: from ancient to recent, Landslides (3 September 2011), 1-10
4. Cundall P A (1971) A computer model for simulating progressive large scale movement in blocky rock systems. Proceedings of the Symposium of the International society of rock mechanics, 1. Nancy, France, II-8.
5. Cundall P A, Strack OD (1979) A discrete numerical model for granular assemblies. Geotechnique 29: 47-65.
6. Dong JJ, Lee WR, Lin ML, Huang AB, Lee YL (2009) Effects of seismic anisotropy and geological characteristics on the kinematics of the neighboring Jiufengershan and Hungtsaiping landslides during Chi-Chi earthquake. Tectonophysics 466(3–4): 438–457
7. Fakhimi A, Villegas T (2007) Application of dmensional anlysis in calibration of a discrete element model for rock deformation and fracture. Rock Mechanics and Rock Engineering 40: 193-211.
8. Itasca, Consulting Group Inc (2002) PFC3D Particle Flow Code in 3 Dimensions. User's Guide. Minneapolis.
9. Lee JF, Wei CY, Huang CC (2004) The study of Hungtsaiping landslide using digital photogrametric technique. Proceeding of International Symposium on Landslide and Debris Flow Hazard Assessment, 2004 Oct 7th–8th, Taiwan, pp. 5–1–5-9.
10. Lee WHK, Shin TC, Kuo KW, Chen KC, Wu CF (1999) CWB free field strong-motion data from the 921 Chi-Chi earthquake: volume 1. Digital Acceleration Files on CD-ROM.

11. Liao HW (2000) Landslides triggered by Chi-Chi earthquake. Master's thesis, Institute of Geophysics, National Central University (in Chinese).
12. Lo CM, Lin ML, Lee WC, Lee KC, Chien SY, Dong JJ, Chang KT, Huang AB (2008) Landslide characterization and zonation of Hungtsaiping area based on topography, aerial photograph and PIV technology. The 3rd International Conference on Site Characterization, Taipei, Taiwan, 1–4 April 2008, pp 467–472 (CD ROM)
13. Lo CM, Lin ML, Tang CL, Hu JC (2011) Kinematic Process of the Xiaolin Catastrophic Landslide, Eng Geol
14. Hoek, E., Carranza-Torres, C. and Corkum, B. (2002), Hoek-Brown Failure Criterion-2002 Edition, 5th North American Rock Mechanics Symposium and 17th Tunneling Association of Canada Conference: NARMS-TAC, pp. 267-271.
15. Poisel R, Roth W (2004) Runout models of rock slope failures. Felsbau 22: 46-50. Poisel R, Bednarik M, Holzer R, LIŠČÁK P (2005) Geomrchanics of Hazardous landslides. Journal of Mountain Science 2(3): 211-217.
16. Potyondy D, Cundall P (2004) A bonded-particle model for rock. International Journal of Rock Mechanics & Mining Sciences 41:1329–1364
17. Steven N W, Simon D (2006) Particulate kinematic simulations of debris avalanches: interpretation of deposits and landslide seismic signals of Mount Saint Helens, 1980 May 18. International Journal of geophysics 167: 991-1004.
18. Tang CL, Hu JC, Lin ML, Angelier J, Lu CY, Chan YC, Chu HT (2009) The Tsaoling landslide triggered by the Chi-Chi earthquake, Taiwan: insights from a discrete element simulation. Eng Geol 106:1–19
19. Wei CY, Lee JF (2006) The application of digital aerial photography in the study of Hungtsaiping landslide, Chungliao, Nantou County. Bulletin of the Central Geological Survey 19: 39–59 (in Chinese).
20. Yoon J (2007) Application of experimental design and optimization to PFC model calibration in uniaxial compression simulation. International Journal of Rock Mechanics & Mining Sciences 44:871–889

地質構造影響歷次紅菜坪地滑運動行為之三維模擬初探

摘要

民國 88 年 9 月 21 日清晨發生「集集大地震」，造成台灣地區的嚴重災情，集集地震造成紅菜坪發生大規模邊坡滑動其面積約 100 公頃之深層滑動災害。經現地調查發現不整合面及位移等證據，得此地為一再發生滑動且滑動機制複雜之古崩塌地，為了解及解釋其崩塌機制綜合野外勘查、地質剖面分析、地電阻及室內物理試驗資料，做為數值模擬參數、三維地質地形建模之依據，以三維分離元素法(PFC^{3D})模擬研究區中民國 5 年至民國 88 年間三起重大歷史山崩事件，以釐清邊坡滑動之歷史情形及機制。

關鍵字：地震、崩塌、分離元素法、模擬。

Table 1. The comparison results of uniaxial compression test by the Hoek–Brown failure criterion and PFC Model.

Item	sandstone mass estimated by the Hoek–Brown failure criterion	PFC Model (Marco-properties)
Density	2,600 kg/m^3	2,600 kg/m^3
Young's Modulus (Ec)	407.21MPa	407.23MPa
UCS	5.249MPa	5.251MPa

Table 2 The numerical parameters of PFC modeling.

	The numerical parameters of compression test	The numerical parameters of the landslide
Number of wall elements	2	87,000
Number of particles	2,650	18,379
Particle density (kg/m^3)	2,600	2,600
Range of particle radius (m)	0.075-0.1	7.5
Normal stiffness (KN/m)	1.42e8	1.22e10
Shear stiffness (KN/m)	0.56e8	0.61e10
Friction coefficient of ball	0.5	0.3
Friction coefficient of wall	0.5	0.3
Normal stiffness of parallel bonds (KN/m^3)	2.39e9	2.71e7
Shear stiffness of parallel bonds (KN/m^3)	1.19e9	1.35e7
Normal strength of parallel bonds (Mpa)	5.2	5.2
Shear strength of parallel bonds (MPa)	2.6	2.6

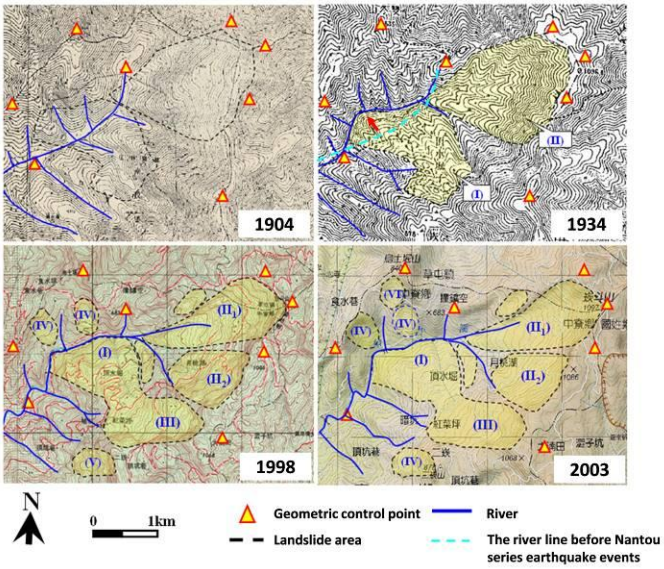

Fig 1. Topographic maps showing the location of the Hungtsaiping landslide

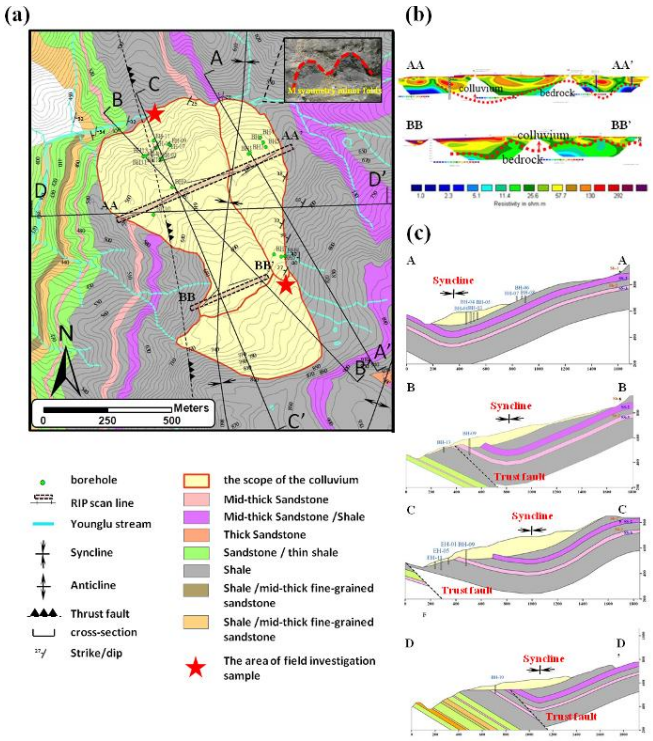

Fig 2. The geology investigation and borehole logs surveying and mapping the underlain strata of Hungtsaiping landslide, and locations of boreholes and resistivity exploration.

a. The geological map of the landslide area.
b. Profile AA-AA' and BB-BB' across the slide directions with resistivity survey lines (Chang et al., 2011).
c. Cross-sections A-A', B-B', C-C', and D-D' show the topography, geological structures and underlain strata (Dong et al., 2009).

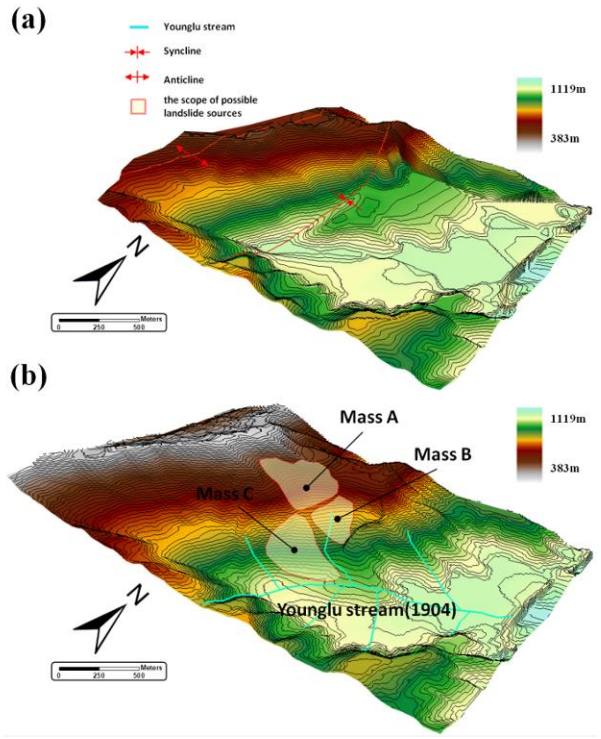

Fig 3. A 3D geological layer, base on the mapping of underlain strata

a. A 3D geological layer of mid-thick sandstone, and include geological structure of syncline and anticline.
b. A 3D geological layer of shale, that reconstructed sliding surface base on **Fig 3. a**., and modified by topographic maps from 1904. And the scope of possible landslide sources: mass A, mass B, massC.

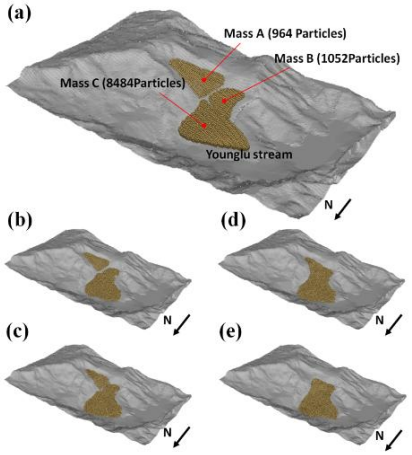

Fig 4. The numerical modeling of the Hungtsaiping landslide.

a. The Hungtsaiping landslide model was constructed using wall and ball elements constructed**.**
b. Simulations of the first landslide event during the Nantou series of earthquake events.
c., d. Simulation of after the Nantou series of earthquake events caused the second landslide event. The mass A lost support, and collapsed under the influence of gravity.
e. Simulation of after the Chi-chi earthquake events caused the ancient landslide movement.

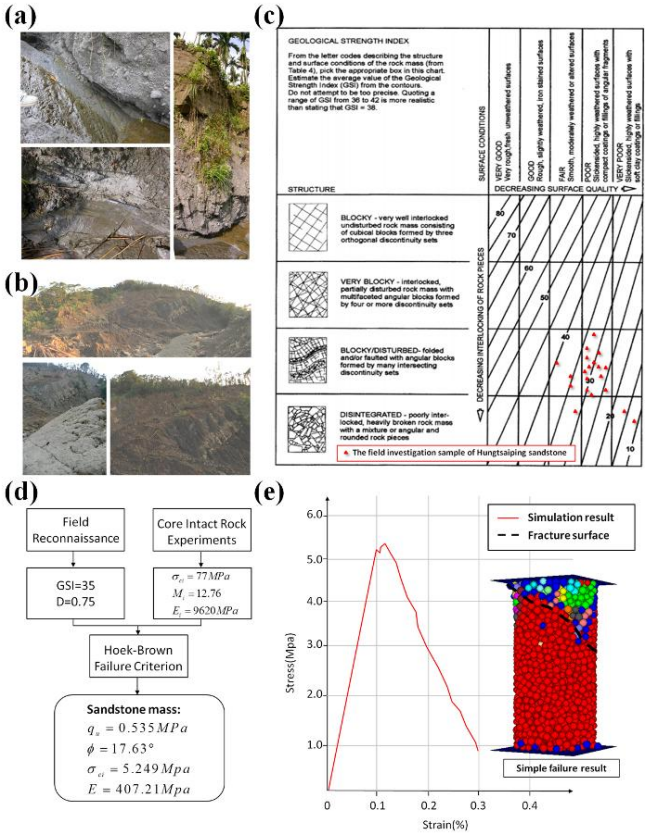

Fig 5. The field investigation sample to modify strength properties of Hungtsaiping sandstone borehole logs result (Chang et al., 2011) by the Hoek–Brown failure criterion and simulation uniaxial compression test..

a. The field investigation area of Fig 2a., the middle of slope.
b. The field investigation area of Fig 2a., the slope toe .
c. The geological strength index and field investigation sample distribution.
d. The intact rock parameter (Mi) determined by fitting the data of Brazilian, uniaxial compression, and triaxial compression tests b Strength properties of

sandstone mass estimated by the Hoek–Brown failure criterion

e. The comparison result of simulation uniaxial compression test.

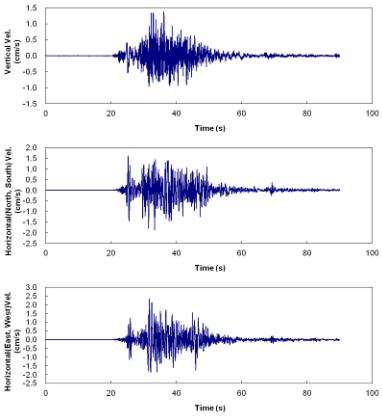

Fig 6. Seismic records at TCU072 in the vertical, North-South, and East-West directions.

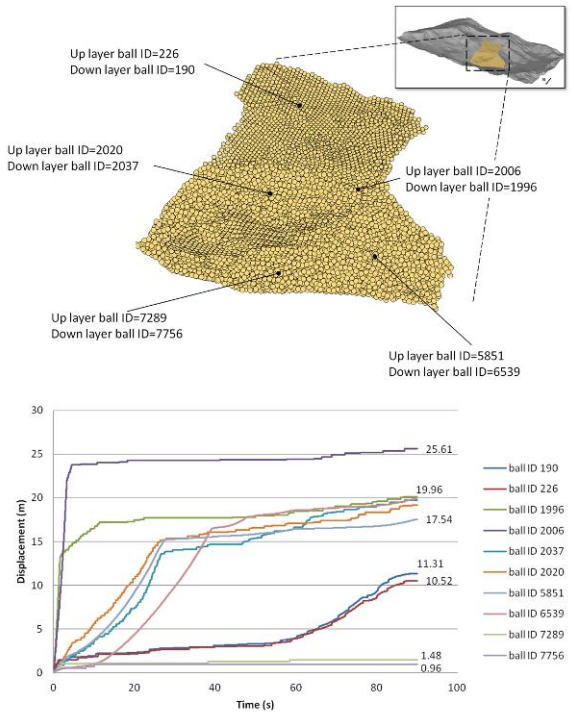

Fig 7. The sliding mass location, and displacement of ball elements.

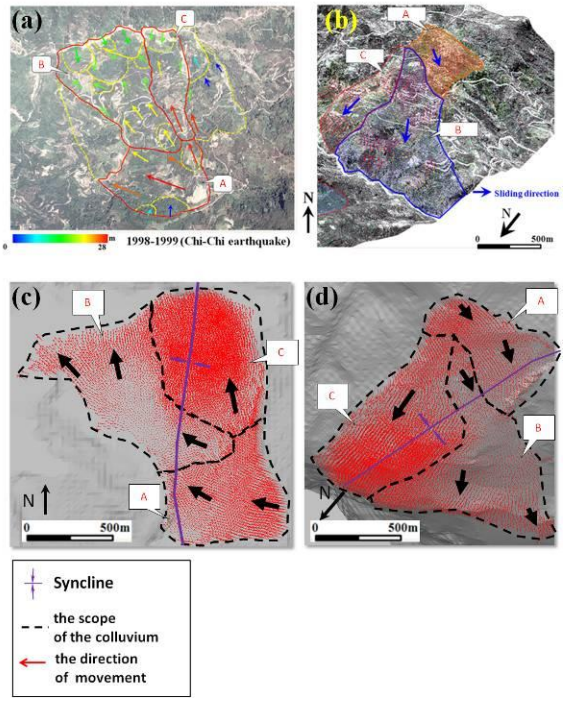

Fig 8. The results of simulation during Chi-chi earthquake events.

a., b. The surface displacement identified morphologic changes by the particle image velocimetry technology (PIV) for detailed landslide zonation with topographic maps (Lo et al., 2008).

c., d. The surface displacements identified by PFC 3D for simulated kinematics of Hungtsaiping landslide.